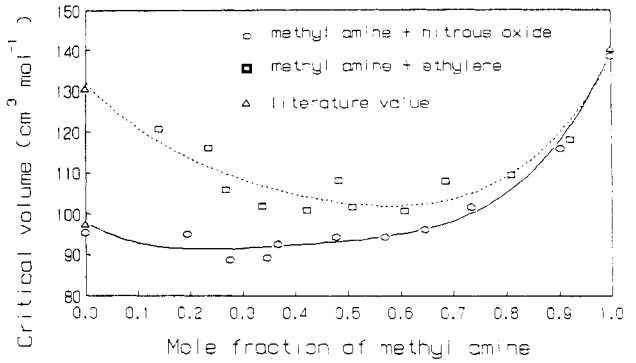

Figure 4. Critical volume as a function of methylamine mole fraction in the systems methylamine + nitrous oxide and methylamine + ethylene.

figures, for both systems the critical lines are continuous over the whole composition range between the critical points of the pure components. The critical pressure passes through a maximum at about 55 and 65 mol % methylamine in its binary mixtures with nitrous oxide and ethylene, respectively. Critical volumes pass through a minimum. The scattering in the critical volume data stems from the difficulty in direct experimental measurement of critical volumes as mentioned above.

Registry No. N_2O, 10024-97-2; CH_3NH_2, 74-89-5; ethylene, 74-85-1.

Literature Cited

(1) Beer, R.; Peter, S. In *Supercritical Fluid Technology*; Penninger, J. M., Radosz, M., McHugh, M. A., Krukonis, V. J., Eds.; Elsevier: New York, 1985; pp 385-396.
(2) Saraf, V. P.; Kiran, E. *Polym. Prepr.* **1987**, *28*(2), 397-398.
(3) Rowlinson, J. S.; Swinton, F. L. *Liquids and Liquid Mixtures*; Butterworths: London, 1982; pp 70-75.
(4) Young, C. L. In *Chemical Thermodynamics—Volume 2*; The Chemical Society: London, 1978; pp 71-104.
(5) Reid, R. C.; Prausnitz, J. M.; Poling, B. E. *The Properties of Gases and Liquids*, 4th ed.; McGraw-Hill: New York, 1987.

Received for review August 31, 1987. Accepted February 8, 1988. This work has in part been supported by the National Science Foundation Grant No. CBT-8416875.

High-Temperature Diffusion, Viscosity, and Density Measurements in *n*-Eicosane

John B. Rodden, Can Erkey, and Aydin Akgerman*

Department of Chemical Engineering, Texas A&M University, College Station, Texas 77843

Taylor dispersion technique is used to measure the infinite dilution diffusion coefficients of eight solutes (H_2, CO, CO_2, *n*-C_8H_{18}, *n*-$C_{10}H_{22}$, *n*-$C_{12}H_{26}$, *n*-$C_{14}H_{30}$, *n*-$C_{16}H_{34}$) in *n*-eicosane over the temperature range 100–260 °C at 1.38 MPa pressure. The density and viscosity of *n*-eicosane were measured at the same conditions as well. It is shown that the rough hard-sphere theory can correctly represent the data.

Introduction

Mutual diffusion coefficients, viscosity, and density are the thermophysical properties needed in evaluation of mass-transfer phenomena and in design of equipment for mass-transfer operations. Diffusion data at high temperatures are very scarce and are nonexistent for high-boiling substances. Our objective is to measure these three thermophysical properties in a homologous series of alkanes. We have reported our measurements of diffusion, viscosity, and density in heptane, dodecane, and hexadecane over a wide temperature range previously (*1*, *2*). This work extends the previous study to *n*-eicosane.

Experimental Techniques

Infinite dilution diffusion coefficients of three gaseous (hydrogen, carbon monoxide, and carbon dioxide) and five alkane (octane, decane, dodecane, tetradecane, and hexadecane) solutes in *n*-eicosane were measured by using the Taylor dispersion technique (*3*). In this method, a narrow pulse of solute (A) diluted in the solvent (B) is injected into a tube in which the solvent is moving in slow laminar flow. The pulse ultimately assumes a Gaussian distribution whose temporal variance σ^2 is dependent on the average velocity $\bar{u}$ and molecular diffusivity D_{AB}. At the end of the diffusion tube the concentration $C(t)$ is recorded as a function of time data as the peak elutes through a detector. The normalized first and second temporal moments ($\bar{t}$ and σ^2) are calculated by finite summation. The following equations result in the direct calculation of the diffusion coefficient.

$$D_{12} = \frac{1}{2}\left[\bar{u}L\zeta_0 - \left[(\bar{u}L\zeta_0)^2 - \left(\frac{\bar{u}^2R^2}{12}\right)\right]^{1/2}\right] \quad (1)$$

where

$$\bar{u} = (L/\bar{t})(1 + 2\zeta_0) \quad (2)$$

$$\zeta_0 = \frac{2\sigma^2 - \bar{t}^2 + [\bar{t}^4 + 4\bar{t}^2\sigma^2]^{1/2}}{(8\bar{t}^2 - 4\sigma^2)} \quad (3)$$

Equation 1 accounts for molecular diffusion in both axial and radial directions within the dispersion tube. The tube length L and the radius R are corrected for thermal expansion effects which are significant at temperatures above 100 °C.

Viscosity is measured with the standard capillary viscometer technique, which is based on the Hagen–Poiseuille equation. Density is measured by a new technique we developed which is based on the retention time of the solute peak (*4*, *5*). The retention time is just the first temporal moment $\bar{t}$ calculated from the Taylor dispersion experiment and it depends on the solvent density, dispersion tube volume V_t, and mass flow rate. The tube volume is calibrated by using a fluid of known density such as water. Thus the density of *n*-eicosane can be calculated from

$$\rho_2 = \rho_1 \frac{\dot{m}^{(2)}\bar{t}^{(2)}V_t^{(1)}}{\dot{m}^{(1)}\bar{t}^{(1)}V_t^{(2)}} \quad (4)$$

* Author to whom inquiries should be addressed.

0021-9568/88/1733-0344$01.50/0

Table I. Diffusion Coefficients of Gases in n-Eicosane at 200 psia ($D_{12} \times 10^9$ m^2/s)

solute	temp, °C	D_{12}(exptl)	D_{12}(predicted by eq 7)
H_2	101.1	16.27 ± 0.98	16.24
	139.3	24.10 ± 0.30	24.14
	176.6	33.53 ± 0.61	33.75
	221.6	46.62 ± 0.77	48.49
	260.3	67.19 ± 3.21	62.98
CO	101.1	6.04 ± 0.07	6.10
	139.3	8.95 ± 0.18	9.07
	176.6	12.23 ± 0.05	12.68
	221.6	17.36 ± 0.35	18.22
	260.3	23.24 ± 0.76	23.67
CO_2	101.1	5.41 ± 0.03	5.13
	139.3	8.05 ± 0.25	7.63
	176.6	10.74 ± 0.06	10.67
	221.6	15.19 ± 0.20	15.33
	260.3	20.02 ± 0.27	19.91

Table II. Diffusion Coefficients of n-Alkanes in n-Eicosane at 200 psia ($D_{12} \times 10^9$ m^2/s)

solute	temp, °C	D_{12}(exptl)	D_{12}(predicted by eq 7)
n-C_8H_{18}	101.8	2.03 ± 0.02	1.69
	140.0	2.98 ± 0.04	3.06
	180.6	4.34 ± 0.01	4.61
	221.3	6.26 ± 0.08	6.59
	260.4	8.58 ± 0.05	8.60
n-$C_{10}H_{22}$	140.0	2.53 ± 0.04	2.65
	221.6	5.59 ± 0.04	5.70
n-$C_{12}H_{26}$	101.8	1.47 ± 0.01	1.30
	139.9	2.29 ± 0.03	2.34
	180.6	3.34 ± 0.02	3.53
	221.5	4.91 ± 0.10	5.05
	260.4	6.72 ± 0.11	6.58
n-$C_{14}H_{30}$	140.0	2.02 ± 0.04	2.11
	221.4	4.46 ± 0.12	4.55
n-$C_{16}H_{34}$	101.8	1.17 ± 0.03	1.07
	139.9	1.94 ± 0.03	1.93
	180.6	2.77 ± 0.00	2.91
	221.6	4.08 ± 0.02	4.16
	260.4	5.55 ± 0.10	5.42

The volume of the dispersion tube $V_t^{(2)}$ is corrected for thermal expansion effects at high temperatures.

The equipment used for the Taylor dispersion experiment is explained by Matthews and Akgerman (*6*). The n-eicosane is heated to 70 °C in a reservoir to keep it in liquid form and is sparged continuously with helium. It is pumped through a heated line that has a capillary restrictor and a back-pressure regulator into a heated enclosure that contains the capillary viscometer. The pressure drop across the capillary is measured with two strain gauge transducers which were calibrated against a Ruska dead weight pressure gauge. The solvent n-eicosane then flows through the reference side of the concentration detector (LDC/Milton Roy Refractomonitor) and back into the heated enclosure where the solute sample is injected via a heated switching valve. The dispersion of the sample peak is then detected at the sample side of the detector.

Hexadecane, decane, and eicosane were obtained from Alfa Chemicals, tetradecane was from MCB Reagents, and dodecane was from Eastman Chemicals. All alkanes and bottled gases were used as received. The minimum purity for all alkanes was 99 mol % which was confirmed by gas chromatography.

Results and Discussion

Diffusion coefficients with the standard deviations are given in Tables I and II. For each diffusivity measurement, three repeat experiments were performed and the results were averaged. A 95% confidence interval of ±5% of the mean is generally sufficient for the data. We have applied the rough hard-sphere theory (RHS) to prediction and correlation of diffusion in alkane/alkane system (*7*). According to this theory, the diffusion coefficient is given by

$$D_{12}/T^{1/2} = \beta(V - V_D) \tag{5}$$

where V is the molar volume, V_D is the close-packed hard-sphere volume for the solvent, and β is a constant which is a function of molecular interactions. According to eq 5 $D_{12}/T^{1/2}$ should vary linearly with the molar volume of the solvent. Table III summarizes the β and V_D values for each solute obtained through linear regression. The V_D values for the alkane solutes and the gaseous solutes were averaged separately to obtain a V_D value for n-eicosane for alkane solutes and for small gaseous solutes. There is a justification for averaging separately since the intercept V_D is also a weak function of solute size (*7*). The β's for each solute can be correlated with the hard-sphere diameter σ.

Table III. Multiplier β and V_D for Solutes

solute	β	V_D, mL/(g mol)
H_2	0.0299	357.6
CO	0.0102	354.2
CO_2	0.0086	351.9
n-C_8H_{18}	0.0039	359.7
n-$C_{10}H_{22}$	0.0037	364.4
n-$C_{12}H_{26}$	0.0032	361.9
n-$C_{14}H_{30}$	0.0029	364.4
n-$C_{16}H_{34}$	0.0026	362.2

Table IV. Core Diameters from Procedure of Bondi

	σ, Å		σ, Å		σ, Å
H_2	2.572	n-C_8H_{18}	6.552	n-$C_{14}H_{30}$	7.809
CO	3.718	n-$C_{10}H_{22}$	7.022	n-$C_{16}H_{34}$	8.148
CO_2	3.968	n-$C_{12}H_{26}$	7.436	n-$C_{20}H_{42}$	8.753

$$\beta = a\sigma_1^b \tag{6}$$

In this equation, σ_1 is the hard-sphere diameter of the solute and a and b are constants. Therefore, the high-temperature behavior of the diffusion coefficients in n-eicosane can be summarized as

$$\frac{10^9 D_{12}}{T^{1/2}} = a\sigma_1^b(V - V_D) \tag{7}$$

where for n-alkane solutes

$$V_D = 362.5, \quad a = 0.228, \quad b = -2.11 \tag{7a}$$

and for dissolved gas solutes

$$V_D = 354.6, \quad a = 0.346, \quad b = -2.66 \tag{7b}$$

Table IV gives the hard-sphere diameters of solutes calculated by using the procedure of Bondi (*8*). Figures 1 and 2 show the data and the plot of eq *7*.

As seen in Figures 1 and 2, there is a slight deviation from linearity. Large deviations from RHS theory may be expected for long-chain hydrocarbons such as n-eicosane since spherical symmetry is highly unlikely. However, the fit to the theoretical equation is surprisingly good considering the size of the molecule. In addition, the deviations from linearity for all the solutes have the same trend which can also be explained in terms of the temperature dependency of the hard-sphere diameters. Due to lack of data to evaluate the temperature dependency of these diameters, we treated them as constants in our analysis.

Viscosity and density of n-eicosane at the operated temperatures and pressure together with the available literature comparison (*9*) are given in Table V. There is no density data above 150 °C at 205 psia. Figure 3 gives a plot of density versus temperature both for our data and the data from the

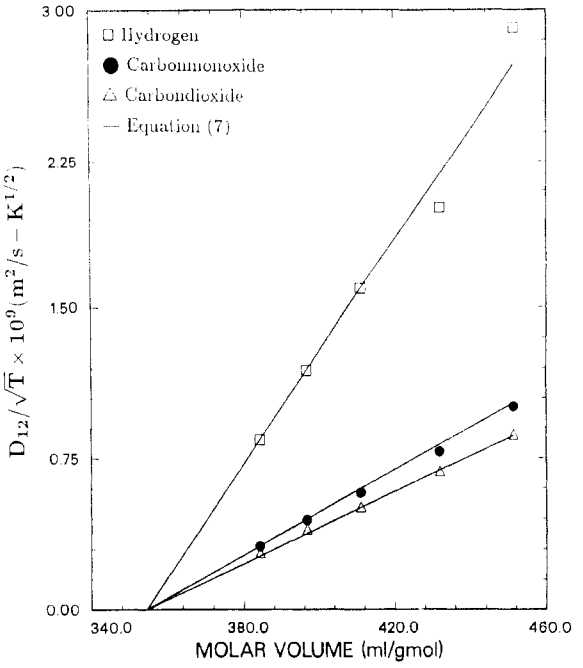

Figure 1. Diffusivities of gases in *n*-eicosane.

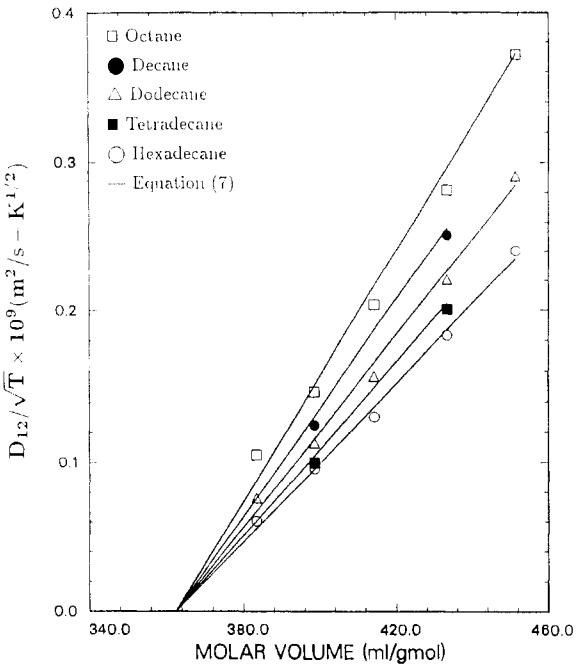

Figure 2. Diffusivities of *n*-alkanes in *n*-eicosane.

Table V. Viscosity and Density of *n*-Eicosane at 200 psia

temp, °C	viscosity, cP		density, g/mL	
	exptl	from ref 9	exptl	from ref 9
101.8	1.446	1.373	0.7351	0.7347
140.1	0.972	0.867	0.7120	0.7090
180.7	0.670	0.591	0.6872	not available
221.6	0.470	0.430	0.6541	not available
261.1	0.338	0.330	0.6259	not available

literature. This work thus provides a modest extension of available data.

The measured viscosity values are also consistent with the RHS approach to viscosity (η). By a development analogous to that for self-diffusion, it has been shown that (*10*)

$$\frac{T^{1/2}}{\eta} = \beta(V - V_\eta) \qquad (8)$$

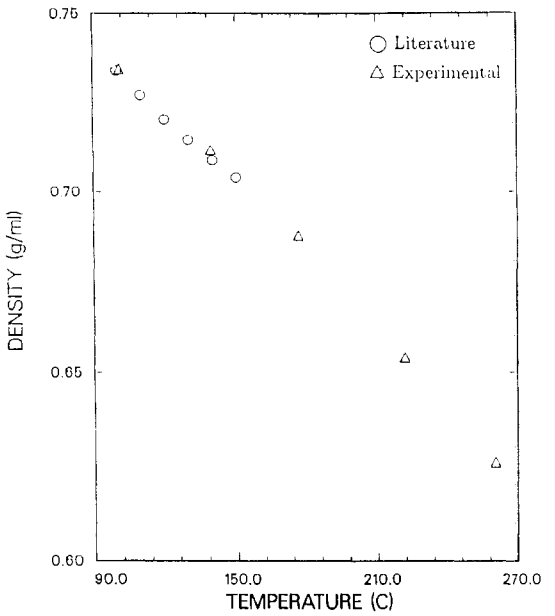

Figure 3. Density of *n*-eicosane as a function of temperature at 1.38 MPa pressure.

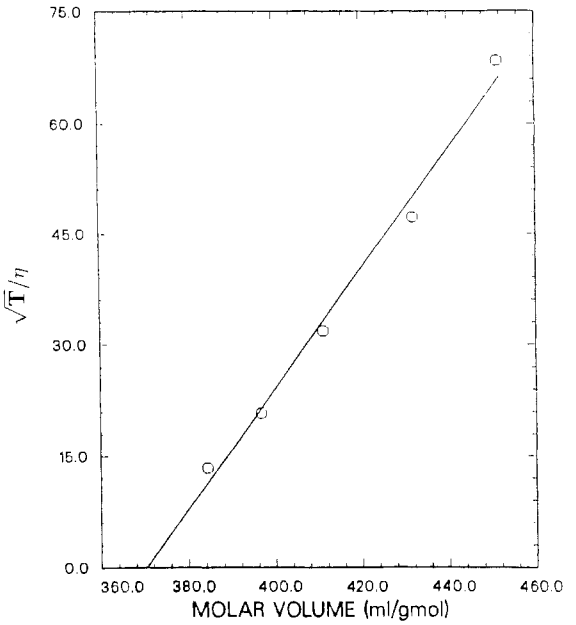

Figure 4. Dependence of $T^{1/2}/\eta$ on molar volume of *n*-eicosane.

The above relation is plotted in Figure 4 for *n*-eicosane. The quantities β' and V_η are analogous to β and V_D. V_η is the molar volume at which the fluidity $1/\eta$ goes to zero. V_η equals 370.2 mL/(g mol) for eicosane and this value is very close to V_D values determined both for gaseous and alkane solutes as predicted by RHS theory. There is again a slight deviation from linearity which may be due to the same factors.

Glossary

D_{12}	diffusivity of solute 1 in solvent 2
L	dispersion tube length
$\dot{m}$	mass flow rate
R	dispersion tube radius
T	absolute temperature
$\bar{t}$	first temporal moment
V	molar volume of solvent
ρ	density
σ^2	second temporal moment
η	viscosity

Registry No. H_2, 1333-74-0; CO, 630-08-0; CO_2, 124-38-9; n-C_6H_{18}, 111-65-9; n-$C_{10}H_{22}$, 124-18-5; n-$C_{12}H_{26}$, 112-40-3; n-$C_{14}H_{30}$, 629-59-4; n-$C_{16}H_{34}$, 544-76-3; n-$C_{20}H_{42}$, 112-95-8.

Literature Cited

(1) Matthews, M. A.; Akgerman, A. *J. Chem. Eng. Data* **1987**, *32*, 317.
(2) Matthews, M. A.; Akgerman, A. *J. Chem. Eng. Data* **1987**, *32*, 319.
(3) Alizadeh, A.; Wakeham, W. A. *Int. J. Thermophys.* **1982**, *3*, 307.
(4) Matthews, M. A.; Akgerman, A. *Int. J. Thermophys.* **1987**, *8*, 363.
(5) Matthews, M. A.; Akgerman, A. *Diffusivities of Synthesis Gas and Fischer-Tropsch Products in Slurry Media*; Quarterly Report, Jan.-Mar. 1986, U. S. Department of Energy DE-AC2284PC 70032.
(6) Matthews, M. A.; Akgerman, A. *AIChE J.* **1987**, *33*, 881.
(7) Matthews, M. A.; Akgerman, A. *J. Chem. Phys.* **1987**, *87*, 2285.
(8) Bondi, A. *J. Phys. Chem.* **1984**, *68*, 441.
(9) *TRC Thermodynamic Tables—Hydrocarbons*; Thermodynamic Research Center, Texas A&M University: College Station, TX, 1986.
(10) Dymond, J. H. *J. Chem. Phys.* **1974**, *60*, 969.

Received for review September 14, 1987. Accepted March 9, 1988. This work was supported by Contract DE-AC22-84PC 70032 from the U.S. Department of Energy.

Nonequilibrium Thermodynamic Studies of Electrokinetic Effects. 20. Electroosmotic Studies of Acetonitrile + Nitromethane Mixtures across a Sintered Disk

R. L. Blokhra,* Satish Kumar, Rajesh Kumar, and Neelam Upadhyay

Department of Chemistry, Himachal Pradesh University, Shimla 171 005, India

Experimental results for electroosmotic velocity and electroosmotic pressure difference for acetonitrile–nitromethane mixtures across a Pyrex sintered disk (G_3) at different compositions, voltages, and temperatures are reported. The results have been interpreted in light of the thermodynamics of irreversible processes. The efficiency of electrokinetic energy conversion (E_e) has also been calculated. The maximum energy conversion took place at half the value of the electroosmotic pressure. The relaxation time τ for all the mixtures has been estimated at different temperatures, and the time dependence of the entropy production has been found to obey Prigogine and Glansdroff's theory of minimum entropy production.

Introduction

Rastogi et al. (*1–5*) and Blokhra et al. (*6–8*) have reported results for electrokinetic effects using a sintered glass disk and a variety of liquids. The workers used the principles of thermodynamics of irreversible process (*9*, *10*) with advantage for treatment of these effects. It was observed earlier that the range of the validity of the theory of thermodynamics of irreversible processes decrease with increase in the dielectric constant (*7*). We have selected an isodielectric mixture of acetonitrile + nitromethane for the present investigation so that there is no variation in the dielectric constant of the liquid phase at different compositions of the constituents of the liquid phase. Further, in our earlier communications (*11*, *12*), we found that acetonitrile is the main contributing component for high electrokinetic energy conversion. The purpose of the present study is to report results of an isodielectric mixture with acetonitrile as one of the constituents so that the role of acetonitrile, if any, could be ascertained in the phenomenon.

Experimental Section

Materials. Acetonitrile (BDH), after keeping over anhydrous calcium oxide for about 48 h, was shaken vigorously with phosphorus pentoxide and was distilled. The first fraction was discarded and the middle fraction was refluxed again over calcium oxide and was refractionated.

Nitromethane (BDH) was first dried by keeping over anhydrous calcium chloride for about 24 h. Then it was purified by simple distillation over fused calcium chloride and was stored in air-tight bottles for the present study.

Results and Discussion

For systems close to equilibrium, the following linear phenomenological relations hold

$$I = L_{11}\Delta\phi + L_{12}\Delta P$$
$$J = L_{21}\Delta\phi + L_{22}\Delta P \qquad (1)$$

where I and J denote the electric current and volume flux, respectively, while $\Delta\phi$ and ΔP are electric potential difference and pressure difference. The phenomenological coefficients L_{11}, L_{12}, L_{21}, and L_{22} relate to electrical conduction, streaming conduction, electroosmosis, and permeation, respectively.

The electroosmotic data have been analyzed as described ealier (*7*). The values of $J_{\Delta P=0}$, $\Delta P_{J=0}$, L_{21}, and L_{22} for different mixtures, 20, 40, 50, 60, and 80% at 298 K and 50% at 303, 308, 313, and 318 K, at different voltages are given in Table I. The volume flow can be written as

$$J_{\Delta P=0} = L_{21}\Delta\phi \qquad (2)$$

Therefore, a plot of $J_{\Delta P=0}$ vs $\Delta\phi$ should give a straight line. Linear relationship between J and $\Delta\phi$ has been found for all the mixtures studied at all temperatures. This linear relationship holds good for voltages between 40 and 260 V. A sample plot of $J_{\Delta P=0}$ vs $\Delta\phi$ (for 40% acetonitrile at 298 K) is shown in Figure 1.

Efficiency of Energy Conversion

Osterle and co-workers (*13–15*), and Kedam and Caplan (*16*), have discussed the efficiency of electrokinetic energy conversion on the basis of nonequilibrium thermodynamics. The phenomenon of electroosmosis flow can be used with advantage in the design of energy conversion devices. In this case, electrical energy is converted into mechanical work.

In general the equation for conversion efficiency E_e, in terms of conjugate fluxes and forces J and X, has been deduced by Osterle as

$$E_e = -\frac{J_o X_o}{J_i X_i} \qquad (3)$$

where subscripts o and i represent the output and input quantities, respectively. The negative sign in eq 3 indicates that

0021-9568/88/1733-0347$01.50/0